PERGAMON

International Journal of Heat and Mass Transfer 45 (2002) 4241–4250

International Journal of HEAT and MASS TRANSFER

www.elsevier.com/locate/ijhmt

Laminar mixed convection boundary layers induced by a linearly stretching permeable surface

Mohamed Ali [a,*], Fahd Al-Yousef [b]

[a] Department of Mechanical Engineering, King Saud University, P.O. Box 800, Riyadh 11421, Saudi Arabia
[b] King Faisal Air Academy, Riyadh, Saudi Arabia

Received 21 May 2001; received in revised form 12 April 2002

Abstract

The boundary layer flow on a linearly moving permeable vertical surface is studied when the buoyancy force assists or opposes the flow. Similarity and local similarity solutions are obtained for the boundary layer equations subject to power law temperature and velocity variation. The effect of various governing parameters, such as Prandtl number Pr, injection parameter d, and the mixed convection parameter $\lambda = Gr_x/Re_x^2$, which determine the velocity and temperature distributions, the heat transfer coefficient, and the shear stress at the surface are studied. The heat transfer coefficient increases as λ assisting the flow for all d for uniformly or linearly heated surface and as Pr increases it becomes almost independent of λ. However, as the temperature inversely proportional to the distance up the surface, the buoyancy has no effects on the heat transfer coefficient. Critical buoyancy parameter values are obtained for vanished shear stress and for predominate natural convection. Critical values are also presented for predominate buoyancy shear stress at the surface for assisting or opposing flow. A closed form analytical solution is also presented as a special case of the energy equation. © 2002 Published by Elsevier Science Ltd.

1. Introduction

A continuously moving surface through an otherwise quiescent medium has many applications in manufacturing processes. Such processes are hot rolling, wire drawing, spinning of filaments, metal extrusion, crystal growing, continuous casting, glass fiber production, and paper production [1–3]. The study of heat transfer and the flow field is necessary for determining the quality of the final products of such processes as explained by Karwe and Jaluria [4,5].

Since the pioneer study of Sakiadis [6] who developed a numerical solution for the boundary layer flow field of a stretched surface, many authors have attacked this problem to study the hydrodynamic and thermal boundary layers due to a moving surface [7–16].

Suction or injection of a stretched surface was introduced by Erickson et al. [17] and Fox et al. [18] for uniform surface velocity and temperature and by Gupta and Gupta [19] for linearly moving surface. Chen and Char [20] have studied the suction and injection on a linearly moving plate subject to uniform wall temperature and heat flux and the more general case using a power law velocity and temperature distribution at the surface was studied by Ali [21]. Recently, Magyari et al. [22] have reported analytical and computational solutions when the surface moves with rapidly decreasing velocities using the self-similar method, and the flow part of the problem was considered analytically by Magyari and Keller [23] for permeable surface moving with a decreasing velocity for velocity parameters $-1/3$ and $-1/2$.

In all papers cited earlier the effect of buoyancy force was neglected and the following papers have taken the buoyancy force into consideration however, suction or injection at the moving surface was relaxed. Such papers are Lin et al. [24] for horizontal isothermal plate moving in parallel or reversibly to a free stream. Also the papers

* Corresponding author. Tel.: +966-1-467-6672; fax: +966-1-467-6652.
E-mail address: mali@ksu.edu.sa (M. Ali).

0017-9310/02/$ - see front matter © 2002 Published by Elsevier Science Ltd.
PII: S0017-9310(02)00142-4

by Karwe and Jaluria [4,5], Kang and Jaluria [25,26] to obtain the buoyancy effects on moving plate in rolling and extrusion processes, in materials processing, casting process, and in channel flow for thermal processing respectively, and it was found that the effect of thermal buoyancy is more significant when the plate is moving vertically upward than when it is moving horizontally. Ingham [27] studied the existence of the solutions of the boundary layer equations of a uniformly moving vertical plate with temperature inversely proportional to the distance up the plate. Laminar mixed convection of uniformly moving vertical surface for different temperature boundary conditions are considered by Ali and Al-Yousef [28,29].

The present paper investigates the effect of mixed convection boundary layer adjacent to a continuously moving upward vertical surface with suction or injection at the surface for general boundary conditions of power law velocity and temperature distributions. However, the analyses are focused on the case of linearly moving surface with various temperature boundary conditions for different Prandtl numbers.

The mathematical formulation of the problem is presented in Section 2, followed by the analytical solutions in Section 3. Numerical solution procedure is presented in Section 4 and results and discussion are reported in Section 5 and finally conclusions are given in Section 6.

2. Mathematical analysis

Consider the steady two-dimensional motions of mixed convection boundary layer flow from a vertically moving upward surface with suction or injection at the surface. For incompressible viscous fluid environment with constant properties using Boussinesq approximation, the equations governing this convective flow are

$$\frac{\partial u}{\partial x}+\frac{\partial v}{\partial y}=0 \tag{1}$$

$$u\frac{\partial u}{\partial x}+v\frac{\partial u}{\partial y}=g\beta(T-T_\infty)+\nu\frac{\partial^2 u}{\partial y^2} \tag{2}$$

$$u\frac{\partial T}{\partial x}+v\frac{\partial T}{\partial y}=\alpha\frac{\partial^2 T}{\partial y^2} \tag{3}$$

subject to the following boundary conditions:

$$\begin{aligned} &u=u_w=U_0x^m, \quad v=v_w(x) && @\ y=0\\ &T-T_\infty=T_w-T=Cx^n && @\ y=0\\ &u\to 0, \quad T\to T_\infty && @\ y\to\infty \end{aligned} \tag{4}$$

It should be mentioned that, positive or negative m indicate that the surface is accelerated or decelerated from the extruded slit respectively. The x coordinate is measured along the moving upward surface from the point where the surface originates, and the y coordinate is measured normal to it (Fig. 1). Positive or negative v imply injection or suction at the surface respectively, and u and v are the velocity components in x and y directions respectively. Similarity solutions arise when

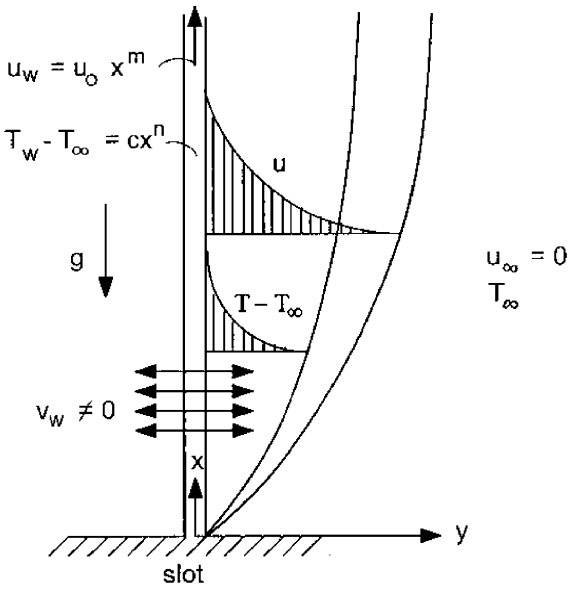

Fig. 1. Schematic of boundary layers induced close to a vertically moving surface.

$$u=U_0x^m f'(\eta), \quad T-T_\infty=Cx^n\theta(\eta) \tag{5}$$

$$\eta=y\sqrt{\frac{m+1}{2}}\sqrt{\frac{U_0x^m}{\nu x}}=\frac{y}{x}\sqrt{\frac{m+1}{2}}\sqrt{Re_x} \tag{6}$$

$$v=-\sqrt{\frac{2\nu U_0}{m+1}}x^{\frac{m-1}{2}}\left(\frac{m+1}{2}f+\frac{m-1}{2}f'\eta\right) \tag{7}$$

where f' and θ are the dimensionless velocity and temperature respectively, and η is the similarity variable. Substitution in the governing equations gives rise to the following two-point boundary-value problem.

$$f'''+ff''-\frac{2m}{m+1}f'^2+\frac{2\lambda\theta}{m+1}=0 \tag{8}$$

$$\theta''+Pr\left(f\theta'-\frac{2n}{m+1}f'\theta\right)=0 \tag{9}$$

The last term in Eq. (8) is due to the buoyancy force and $\lambda=Gr_x/Re_x^2$ which serves as the buoyancy parameter, when $\lambda=0$ the governing equations reduce to those of forced convection limit Ali [12,21]. On the other hand, if λ is of a significantly greater order of magnitude than one, the buoyancy force effects will predominate and the flow will essentially be free convective. Hence, combined convective flow exists when $\lambda=O(1)$. A consideration of Eq. (8) shows that λ is a function of x. Therefore, the

necessary and sufficient condition for the similarity solutions to exist is that $n = 2m - 1$ for f and θ be expressed as functions of η alone. Furthermore, if the above condition is not satisfied, local similarity solutions are obtained (see [30,31]). In this paper similarity solutions are obtained for $m = n = 1$ and local similarity solutions are also found for $m = 1$ at $n = -1$ and 0.

$$f'(0) = 1, \quad f(0) = -v_w\sqrt{\frac{x^{1-m}}{vU_0}}\sqrt{\frac{2}{m+1}},$$

$$f'(\infty) \to 0 \tag{10}$$

$$\theta(0) = 1, \quad \theta(\infty) \to 0 \tag{11}$$

In driving the second of the boundary conditions (10) the horizontal injection or suction speed v_w must be a function of the distance (for $m \neq 1$) from the leading edge. Consequently, v_w can be rewritten as

$$v_w = du_w Re^{-1/2} \quad \text{or} \quad d = \frac{v_w}{u_w}Re^{1/2} \tag{12}$$

in order to have a similarity solution in which the mathematical solution contains η alone. It should be mentioned that, v_w must be of order of magnitude of $u_w Re_x^{-1/2}$ [32], where $Re_x = u_w x/v$, in order to insure that a flow with suction or blowing at the surface satisfies the boundary layer assumptions. Therefore, d that is introduced, as a blowing or suction parameter must be of order one [33]. The second of the boundary conditions (10) can be written as

$$f(0) = -d\sqrt{\frac{2}{m+1}} \tag{13}$$

Eq. (12) shows that, suction or blowing parameter d is used to control the strength and direction of the normal flow at the boundary. Therefore, for positive or negative d we have a blowing or suction boundary condition respectively. Eqs. (8) and (9) reduce to Eqs. (12) and (13) in [27] for $m = 0$, and $n = -1$. Expression for shear stress can be developed from the similarity solution in the form

$$\tau = \mu U_0 x^{m-1}\sqrt{\frac{m+1}{2}}Re^{1/2}f''(\eta) \tag{14}$$

The shear stress can be expressed in a dimensionless form of the skin friction coefficient as

$$C_f = \frac{\tau}{0.5\rho u^2(x)} = \frac{2f''(\eta)\sqrt{0.5(m+1)}}{\sqrt{Re_x}}$$

$$\text{or} \qquad C_f\sqrt{Re_x} = 2f''(\eta)\sqrt{0.5(m+1)} \tag{15}$$

Eq. (15) describes the skin friction coefficient distribution in the boundary layer and its particular value $0.5C_f\sqrt{Re_x} = f''(0)$ for $m = 1$ presents the value on the moving surface. The local heat transfer coefficient h can be expressed in dimensionless form of Nusselt number as

$$\frac{Nu_x}{\sqrt{Re_x}} = -\sqrt{\frac{m+1}{2}}\theta'(0) \tag{16}$$

and for $m = 1$ it is given by $Nu_x/\sqrt{Re_x} = -\theta'(0)$.

3. Analytical solution

The heat transfer part of the problem presented by Eq. (9) exhibit an exact closed form solution in terms of η corresponding to special value of the temperature exponent n such that

$$2n = -(m+1), \quad m > -1 \tag{17}$$

The energy equation (9) for this particular case leads to

$$\theta'' + Pr(f\theta' + f'\theta) = 0 \tag{18}$$

Having in mind the boundary conditions first and third of (10), (11) and (13) one can obtain for any Pr

$$\theta'(0) = -Prf(0) = Prd\sqrt{\frac{2}{m+1}} \quad \text{and}$$

$$\frac{Nu_x}{\sqrt{Re_x}} = -Prd \tag{19}$$

The wall curvature $\theta''(0)$ of the temperature profile can be obtained from Eq. (9) with the parameter values (17) taking into account Eq. (19) by the following simple expression

$$\theta''(0) = Pr\left(\frac{2}{m+1}Prd^2 - 1\right) = -Pr + [\theta'(0)]^2 \tag{20}$$

Eqs. (19) and (20) show that, for any specific value of d, expressed in terms of Pr, the curvature is Prandtl number dependent only for fixed values of m and n given by Eq. (17). These analytical results have been confirmed for $m = 1$ and $n = -1$ by detailed numerical calculations that will be discussed in Section 5. It should be mentioned that, Similar analytical solutions have been found by Magyari and Keller [23] for $m = -1/3, -1/2$, and 1 and by Gupta and Gupta [19] for $m = 1$ for no buoyancy force. Recently, some exact analytical solutions have developed by Magyari et al. [22] for permeable surfaces stretched with rapidly decreasing velocities ($m < -1$).

4. Numerical solution procedure

The coupled nonlinear ordinary differential equations (8) and (9) are solved numerically by using the fourth order Runge–Kutta method. Solutions of the differential equations (8) and (9) subject to the boundary conditions first and third of (10) and (11), and the modified boundary condition (13) were obtained for increasing values of λ at each constant d. At each new d we start from a known solution of the equations with $\lambda = 0$

[12,21] where $f''(0)$ and $\theta'(0)$ are known. For a given value of λ the values of $f''(0)$ and $\theta'(0)$ were estimated and the differential equations (8) and (9) were integrated until the boundary conditions at infinity $f'(\eta)$ and $\theta(\eta)$ decay exponentially to zero (at least of order 10^{-4}). If the boundary conditions at infinity are not satisfied then the numerical routine uses a half interval method to calculate corrections to the estimated values of $f''(0)$ and $\theta'(0)$. This process is repeated iteratively until exponentially decaying solution in f' and θ are obtained. The value of η_∞ was chosen as large as possible depending upon the Prandtl number and the injection parameter d, without causing numerical oscillations in the values of f', f'', and θ. The same procedure was repeated for negative λ where the buoyancy is in the opposite direction to the flow and opposes it. The maximum and minimum λ were obtained for different values of $-0.6 \leqslant d \leqslant 0.6$ where the numerical solutions became more difficult to obtain as λ approached $\lambda_{\max}$ or $\lambda_{\min}$ for the corresponding d. Comparison is made with the available published data in terms of $f''(0)$ and $\theta'(0)$ which show a good agreement with the present results.

5. Results and discussion

Eqs. (8) and (9) were solved numerically, as described in Section 4, for $m = 1$, $d = -0.6$ to 0.6 with a step of 0.2, $Pr = 0.72$, 3, 10, and for temperature exponent $n = -1$, 0, and 1. Samples of the resulting velocity and temperature profiles for $m = 1$, $n = -1$, $d = -0.6$, 0.6, for $Pr = 0.72$, and for different values of λ are presented in Fig. 2(a) and (b). It can be seen that the presence of positive buoyancy (assisting flow) results in a relative rise in the velocity profile near the wall in Fig. 2(a). It is also clear that, the velocity gradient at the surface increases from negative value (opposing flow) passing by that at zero buoyancy force ($\lambda = 0$) to a positive value (assisting flow). The specific critical values of $\lambda = \lambda_{(\text{crt.})s} = 2.2695$, 1.0815 in Fig. 2(a) are for zero velocity gradient where the surface shear stresses are vanished. Table 1 shows these critical values for various values of d and for $n = -1$, 0, and 1. Furthermore, as λ increases, the velocity gradient at the wall for both injection and suction are almost identical which means the flow is predominated by the buoyancy effects. It should be noted that, the hydrodynamic boundary layer thickness in Fig. 2(a) is smaller for $d = -0.6$ than for $d = 0.6$ since the earlier is for suction while the later is for injection.

Fig. 2(b) shows the temperature profiles for the same parameters used in Fig. 2(a). It is clear that as λ increases the thermal boundary layer thickness decreases however, the temperature gradient at the surface is unchanged by changing λ either for suction or injection, resulting in a constant heat transfer rate corresponding to each d independent of λ. This special case is proved analytically

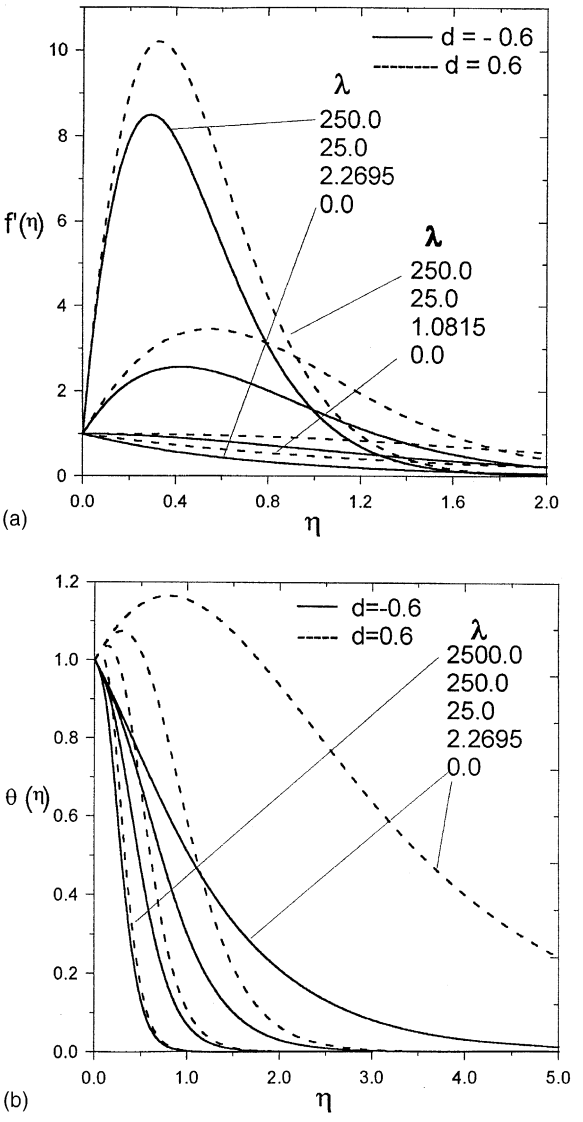

Fig. 2. Samples of velocity and temperature profiles for $Pr = 0.72$, $n = -1$ and $m = 1$ showing the buoyancy effects: (a) velocity, (b) temperature.

in Section 3 for $m = 1$, $n = -1$ and for any Prandtl number and it is confirmed here in Fig. 3(a) where the dimensionless $Nu_x Re_x^{-1/2}$ is independent of λ but it is only function of the suction/injection parameter d. Similar results are obtained for the other Prandtl numbers. Local Nusselt number distributions for $d = -0.6$ and 0.6 and for different values of Prandtl numbers are shown in Fig 3(b). In this figure, it is cleat that $Nu_x Re_x^{-1/2}$ is independent of λ and its negative value means that heat is transferred from the ambient medium to the surface. Furthermore, increasing Prandtl number enhances the heat transfer coefficient for the suction case

Table 1
Critical values of buoyancy parameter $\lambda_{(crt.)s}$ corresponding to vanished shear stresses at the surface at $n = -1$, 0, and 1, for $Pr = 0.72$, 3, and 10.0, and for various values of d

d	$n = -1$			$n = 0$			$n = 1$		
	$Pr = 0.72$	$Pr = 3$	$Pr = 10$	$Pr = 0.72$	$Pr = 3$	$Pr = 10$	$Pr = 0.72$	$Pr = 3$	$Pr = 10$
−0.6	2.2695	4.745	11.00	2.6735	5.5225	12.235	3.011	6.2075	13.335
−0.4	1.994	3.7625	7.909	2.3964	4.5536	9.217	2.7250	5.2069	10.339
−0.2	1.7535	2.938	5.385	2.1560	3.742	6.782	2.4743	4.397	7.9374
0.0	1.545	2.256	3.4025	1.9581	3.07658	4.892	2.264	3.7238	–
0.2	1.3665	1.700	1.9375	1.7807	2.542	3.5065	2.078	3.14465	–
0.4	1.2125	1.2585	0.9585	1.630	2.1252	2.550	1.912	2.698	–
0.6	1.0815	0.912	0.3955	1.505	1.798	1.947	1.7735	–	–

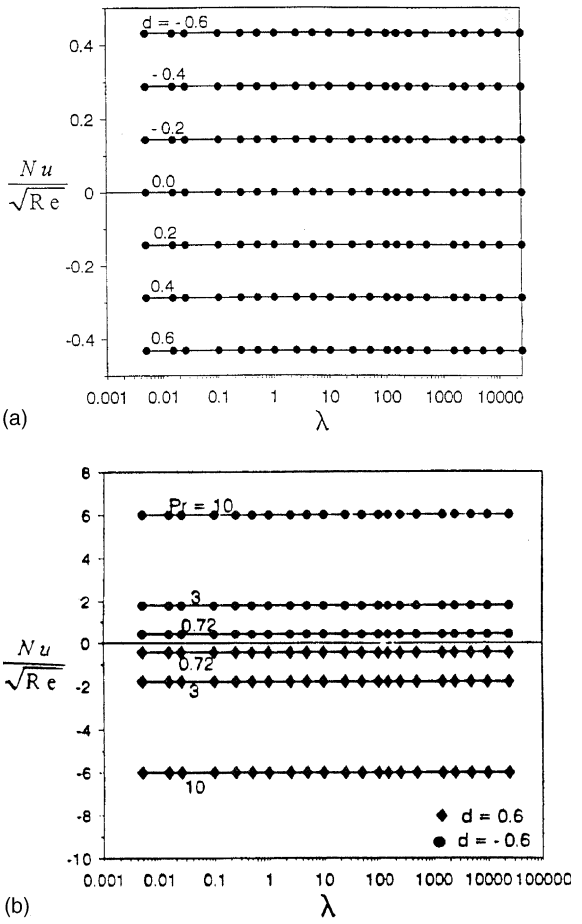

Fig. 3. Local Nusselt number distribution for $m = 1$ and $n = -1$ showing the independence of λ: (a) $Pr = 0.72$, (b) comparison of Prandtl numbers.

but reduces it for the blowing one. It worth mentioning that, the numerical solution for this case can be obtained for any values of λ.

Velocity and temperature profiles for uniform surface temperature ($n = 0$), $Pr = 3.0$, $d = -0.6$ and 0.6 and for various values of λ are shown in Fig. 4(a) and (b). These profiles are similar to those for $Pr = 0.72$ however, the velocities overshoot are moderate at the corresponding maximum λ. For examples: at $d = -0.6$ the maximum λ is 500 (not shown) and the velocity overshoot is 480% however, for $d = 0.6$ the maximum λ is 150 with overshoot of 350%. The corresponding values of $\lambda_{(crt.)s}$ where the shear stress is zero are 5.5225 at $d = -0.6$ and 1.8 at $d = 0.6$ (see Table 1 for other d). Fig. 4(b) show the temperature profiles for the same parameters given in Fig. 4(a). In this figure as λ increases the thermal boundary layer thickness decreases and the temperature gradient at the surface decreases (in contrast to the previous case of $n = -1$ in Fig. 2(b)) hence, the heat transfer rate is enhanced as λ increases for both suction and injection. Furthermore, the suction temperature profiles are squeezed together with reduced thermal boundary layer thickness than that for injection therefore, suction enhances the heat transfer coefficient from the stretched surface than injection.

Fig. 5(a) and (b) shows the velocity and temperature profiles at $\lambda = 25$, $m = 1$, and $d = -0.6$ for different Prandtl numbers and temperature exponents. These figures indicate that increasing Pr and n reduce the hydrodynamic and thermal boundary layers that in turn reduce the shear stress and increase the heat transfer coefficient at the surface respectively.

The local Nusselt number distribution for different values of d, for $Pr = 0.72$ is shown in Fig. 6 for the entire mixed convection regime in terms of $Nu_x Re_x^{-1/2}$ versus λ on a logarithmic scale for $m = 1$ and $n = 0$. The right hand side of the figure presents positive λ on the x-axis where buoyancy assisting flow however, the left side presents the negative λ where buoyancy opposing flow. It is clear from this figure that the heat transfer coefficient increases as d decreases in other words that, suction enhances the heat transfer coefficient while injection reduces it comparing to the impermeable surface ($d = 0$) for fixed λ. Furthermore, as λ increases the heat transfer

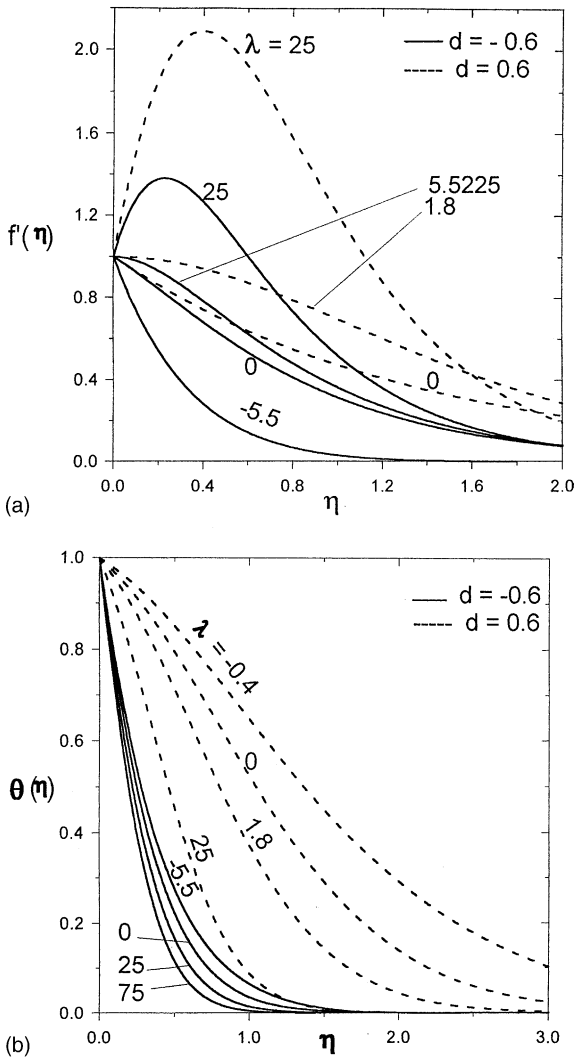

Fig. 4. Samples of velocity and temperature profiles for $Pr = 3$, $n = 0$, and $m = 1$ showing the buoyancy effects: (a) velocity, (b) temperature.

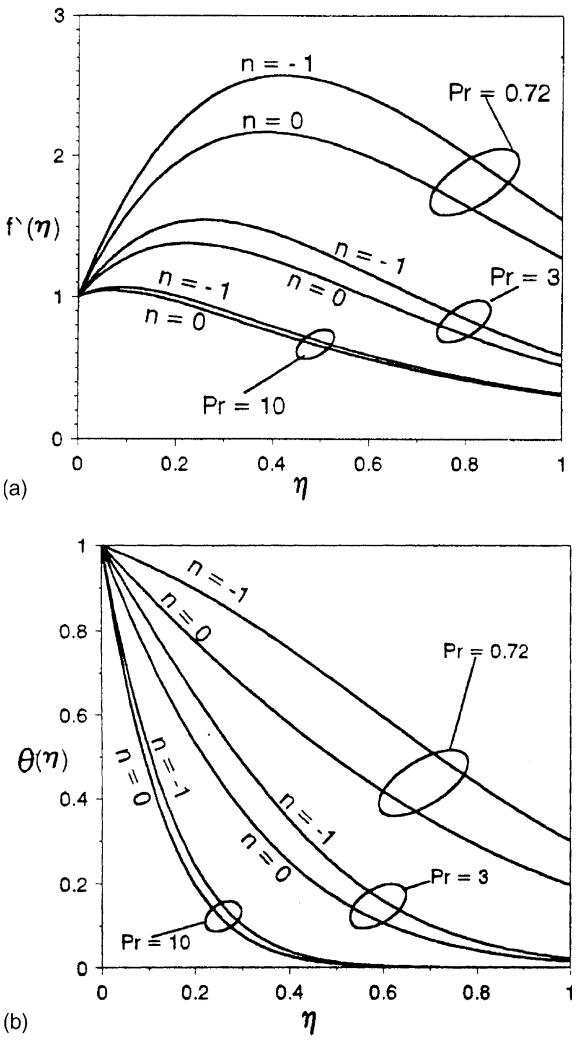

Fig. 5. The effect of Prandtl number and the temperature exponent n for $m = 1$, $d = -0.6$ and for $\lambda = 25$: (a) velocity, (b) temperature.

coefficient increases for fixed d this means, more heat is transferred from the surface to the medium and this quantity of heat is larger for suction than injection at fixed λ. However, at $\lambda > 1000$ where the buoyancy dominates there are no significant differences in $Nu_x Re_x^{-1/2}$ for various values of d and it almost λ dependent only then, the flow is essentially be free convective ($\lambda \gg O(1)$). Moreover, to see the region of predominate natural convection for buoyancy assisting flow, a 5% increase in Nusselt number of that of forced convection limit has been applied. The corresponding values of λ (which we call it critical values $\lambda_{(crt.)c}$) are tabulated in Table 2 for each d. These critical values are presented as solid circles and connected by a dashed line in the figure. Therefore, the region on the right of the dashed line presents the region of natural convection dominates whereas the region on the left presents the domain of forced convection. It should be mentioned that, the entire solutions are presented in this figure however, more solutions can be obtained with buoyancy assisting or opposing flow with lower accuracy and have been rejected.

The distributions of $Nu_x Re_x^{-1/2}$ for $n = 0$, for three values of Pr (0.72, 3, and 10), and for $d \leqslant 0$ are presented in Fig. 7(a). In this figure the upper solid lines are for $Pr = 10$, and the lower solid lines are for $Pr = 0.72$ and the dashed lines are for $Pr = 3$. This figure indicates that,

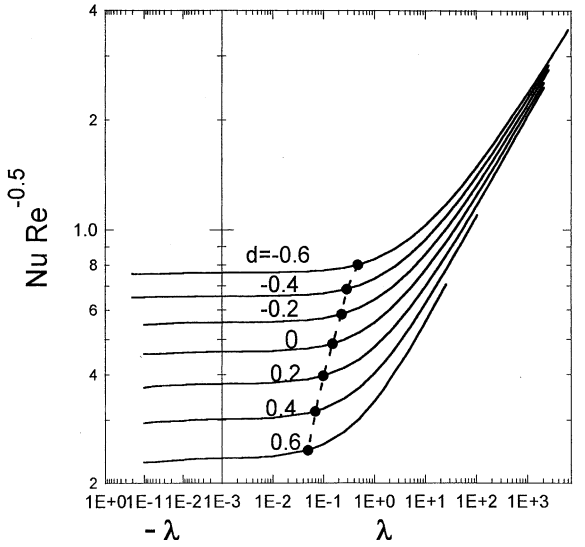

Fig. 6. Local Nusselt number distribution for the entire mixed convection at $n = 0$ for $Pr = 0.72$. Dashed line presents the locus separating the natural convection dominant region on the right and the forced convection region on the left.

for the suction case increasing Pr enhances the heat transfer coefficient since the boundary layer thickness getting smaller and the temperature gradient at the wall getting steeper. Fig. 7(b) shows $Nu_x Re_x^{-1/2}$ distributions for $d > 0$ (blowing), for $Pr = 0.72$, 3 and 10, and for $n = 0$. In this figure as in Fig. 7(a) increasing Pr enhance the heat transfer coefficient however, this enhancement depend on d and Pr. For $d = 0.2$ the effect of increasing Pr is clear but for $d > 0.2$, there is a competition between the injected fluid and the heat transfer for each Pr. The injected fluid increases the boundary layer thickness and the temperature gradient at the wall and make it more flatter and hence reduce the heat transfer. The reduction of $Nu_x Re_x^{-1/2}$ with increasing Pr is more significant for $d > 0.2$.

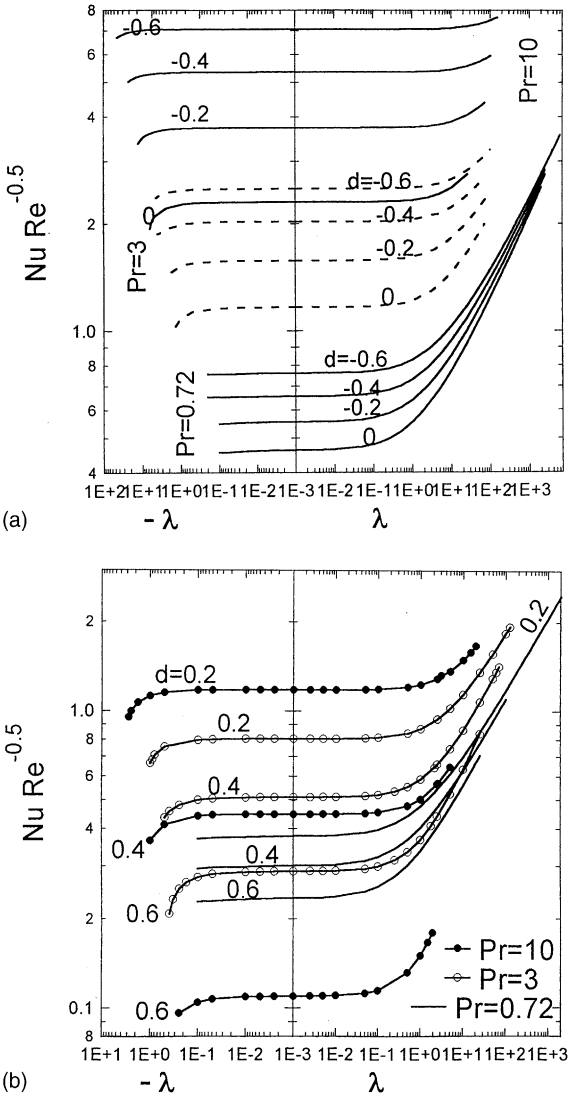

Fig. 7. Local Nusselt number distributions showing the effect of Prandtl number and λ for $n = 0$: (a) $d \leqslant 0$, (b) $d > 0$.

Table 2
Critical values of buoyancy assisting flow $\lambda_{(crt.)c}$ for predominate natural convection at $n = 0$ and 1, for $Pr = 0.72$, 3, and 10.0, and for various values of d

d	$n = 0$			$n = 1$		
	$Pr = 0.72$	$Pr = 3.0$	$Pr = 10.0$	$Pr = 0.72$	$Pr = 3.0$	$Pr = 10.0$
−0.6	0.480	8.200	85.00	0.500	6.30	–
−0.4	0.285	4.000	37.00	0.450	5.10	–
−0.2	0.225	2.430	10.00	0.400	2.49	–
0.0	0.150	1.540	4.750	0.320	2.43	–
0.2	0.100	0.473	1.250	0.255	2.15	–
0.4	0.085	0.165	0.450	0.220	1.40	–
0.6	0.0325	0.124	0.150	0.153	1.32	–

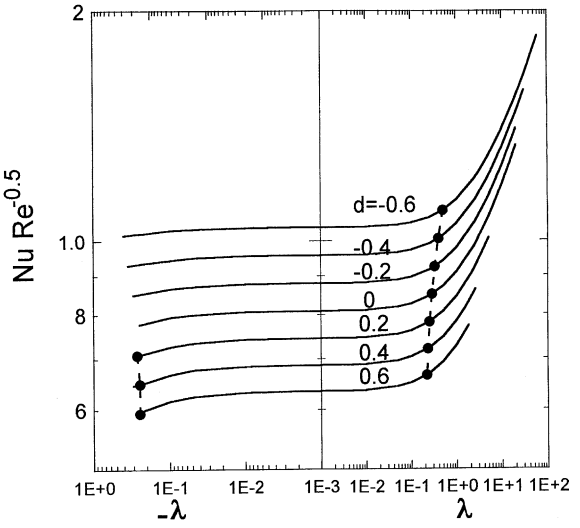

Fig. 8. Local Nusselt number distribution for the entire mixed convection for $Pr = 0.72$ and $n = 1$. The dashed lines present the predominate natural convection for assisting flow (right) and for opposing flow (left).

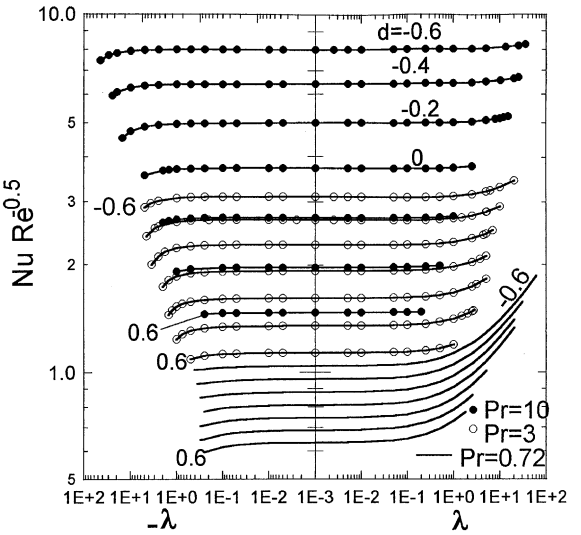

Fig. 9. Local Nusselt number distributions showing the effect of Prandtl number, d and λ for $n = 1$.

The effect of linearly increasing surface temperature ($n = 1$) is shown in Fig. 8 for $Pr = 0.72$ for the same parameter as in Fig. 6(a). The right dashed line separates the region of predominate natural convection on the right and the region of forced convection dominates on the left for buoyancy assisting flow. The left dashed line connecting the points of 5% decrease in $Nu_x Re_x^{-1/2}$ in order to obtain $\lambda_{(\mathrm{crt.})\mathrm{c}}$ for buoyancy opposing flow. It should be noted that, critical points for $d \leqslant 0$ cannot be obtained with reasonable accuracy and are not included in the figure. Table 3 shows the critical values $\lambda_{(\mathrm{crt.})\mathrm{c}}$ for buoyancy opposing flow for other Prandtl numbers for different d and n.

Fig. 9 presents the distributions of $Nu_x Re_x^{-1/2}$ for various Prandtl numbers and d for $n = 1$. In this figure increasing Pr for fixed d and for any λ enhances the heat transfer coefficient and for specific Pr suction always enhances the heat transfer whereas, blowing reduces it. Furthermore, the effect of buoyancy is significant for $Pr = 0.72$ (air) due to the lower density of air that makes it more sensitive to the buoyancy forces.

The dimensionless shear stress at the surface presented by $f''(0)$ for assisting or opposing flow for $n = 0$ and for $Pr = 0.72$ is shown in Fig. 10. A 5% increase or decrease in $f''(0)$ at $\lambda = 0$ has been applied for buoyancy assisting or opposing flow respectively. The two solid lines connecting circles and squares present those values of 5% increase or decrease respectively. The predominate buoyancy effect region is on the right of these two lines. The numerical values of λ which we call it $\lambda_{(\mathrm{crt.})\mathrm{sh}}$ corresponding to these points are given in Tables 4 and 5 for different parameters and for buoyancy assisting or opposing flow respectively. It worth noted that, at large λ where buoyancy dominated there are no significant

Table 3
Critical values of buoyancy opposing flow $\lambda_{(\mathrm{crt.})\mathrm{c}}$ for predominate natural convection at $n = 0$ and 1, for $Pr = 0.72$, 3, and 10.0, and for various values of d

d	$n = 0$			$n = 1$		
	$Pr = 0.72$	$Pr = 3.0$	$Pr = 10.0$	$Pr = 0.72$	$Pr = 3.0$	$Pr = 10.0$
−0.6	–	−4.187	−43.4	–	−4.12	−37.0
−0.4	–	−2.527	−20.4	–	−2.83	−19.7
−0.2	–	−1.47	−8.6	–	−1.93	−10.2
0.0	–	−0.81	−3.17	–	−1.31	−5.2
0.2	–	−0.42	−1.03	−0.27	−1.01	−2.4
0.4	–	−0.21	−0.35	−0.25	−0.72	−1.6
0.6	–	−0.11	−0.107	−0.25	−0.60	–

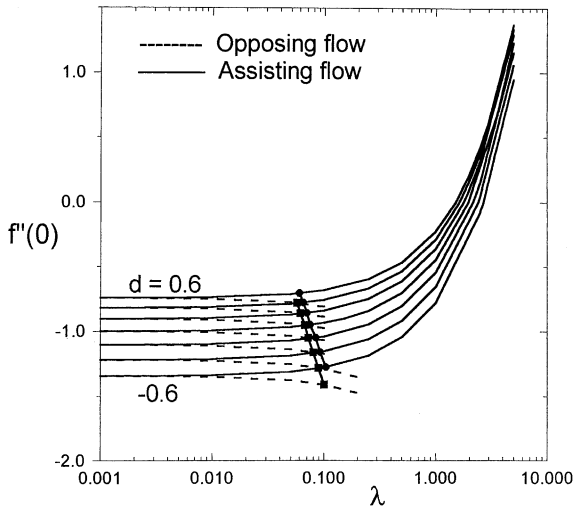

Fig. 10. Dimensionless shear stress distributions at the surface for assisting flow (—) and for opposing flow (– – –). Lines connecting solid circles and squares indicate the predominate buoyancy shear stress for assisting and opposing flow respectively.

differences in $f''(0)$ for various values of d and it turns out that $f''(0)$ is λ dependent only. Similar curves are obtained for $n = -1$ and 1 and for other Prandtl numbers.

6. Conclusions

Heat transfer and flow field characteristics of a linearly moving vertical permeable surface are studied when buoyancy assisting or opposing flow.

The results show that as λ increases (assisting flow) the hydrodynamic and thermal boundary layers thickness decrease however, for opposing flow ($\lambda < 0$) they increase. On the other hand, for uniformly or linearly heated surface ($n = 0$, 1) increasing λ enhances the heat transfer coefficient for all d for $Pr = 0.72$ and 3 but almost has no effect for $Pr = 10$. However, for inversely proportional surface temperature ($n = -1$) the heat transfer coefficient is independent of λ and is suction/injection parameter dependent only for fixed Prandtl number and n. Furthermore, in all cases suction always enhances the heat transfer coefficient over that of blowing for fixed λ. Critical values of buoyancy parameter are obtained for both zero shear stress at the surface and for predominate natural convection for assisting or opposing flow.

At large λ the dimensionless shear stress at the wall is λ dependent only. Critical values of λ corresponding to predominate buoyancy effects on the dimensionless shear stress for assisting or opposing flow are tabulated for different parameters.

Finally, a closed form analytical solution is obtained for the special case of $2n = -(m+1)$ and it is confirmed computationally for $n = -1$ and $m = 1$ where the

Table 4
Critical values of $\lambda_{(crt.)sh}$ for buoyancy assisting flow for predominate buoyancy shear stress at the surface for $n = -1$, 0, and 1, for $Pr = 0.72$, 3, and 10.0, and for various values of d

d	$n = -1$			$n = 0$			$n = 1$		
	$Pr = 0.72$	$Pr = 3$	$Pr = 10$	$Pr = 0.72$	$Pr = 3$	$Pr = 10$	$Pr = 0.72$	$Pr = 3$	$Pr = 10$
−0.6	0.091	0.2250	0.545	0.104	0.260	0.600	0.116	0.290	0.650
−0.4	0.080	0.1760	0.389	0.092	0.210	0.500	0.105	0.238	0.500
−0.2	0.069	0.1350	0.262	0.084	0.170	0.330	0.096	0.199	0.380
0.0	0.060	0.1010	0.163	0.075	0.137	0.230	0.088	0.168	0.284
0.2	0.054	0.0750	0.089	0.070	0.110	0.160	0.080	0.140	0.215
0.4	0.048	0.0530	0.040	0.065	0.091	0.110	0.077	0.120	0.165
0.6	0.042	0.0356	0.013	0.060	0.077	0.085	0.072	0.103	0.130

Table 5
Critical values of $\lambda_{(crt.)sh}$ for buoyancy opposing flow for predominates buoyancy shear stress at the surface for $n = -1$, 0, and 1, for $Pr = 0.72$, 3, and 10.0, and for various values of d

d	$n = -1$			$n = 0$			$n = 1$		
	$Pr = 0.72$	$Pr = 3$	$Pr = 10$	$Pr = 0.72$	$Pr = 3$	$Pr = 10$	$Pr = 0.72$	$Pr = 3$	$Pr = 10$
−0.6	−0.090	−0.223	−0.539	−0.100	−0.255	−0.600	−0.112	−0.285	−0.650
−0.4	−0.077	−0.174	−0.382	−0.089	−0.205	−0.500	−0.098	−0.237	−0.500
−0.2	−0.068	−0.134	−0.256	−0.080	−0.168	−0.330	−0.091	−0.199	−0.380
0.0	−0.060	−0.0998	−0.156	−0.072	−0.135	−0.230	−0.084	−0.160	−0.284
0.2	−.0535	−0.072	−0.083	−0.067	−0.108	−0.160	−0.077	−0.138	−0.211
0.4	−.0479	−0.050	−0.0355	−0.061	−0.087	−0.110	−0.072	−0.116	−0.155
0.6	−0.044	−0.033	−0.011	−0.057	−0.073	−0.083	−0.070	−0.103	−0.120

temperature inversely proportional to the distance up the surface.

References

[1] T. Altan, S. Oh, H. Gegel, Metal Forming Fundamentals and Applications, American Society of Metals, Metals Park, OH, 1979.

[2] E.G. Fisher, Extrusion of Plastics, Wiley, New York, 1976.

[3] Z. Tadmor, I. Klein, Engineering Principles of Plasticating Extrusion, in: Polymer Science and Engineering Series, Van Nostrand Reinhold, New York, 1970.

[4] M.V. Karwe, Y. Jaluria, Fluid flow and mixed convection transport from a moving plate in rolling and extrusion processes, ASME J. Heat Transfer 110 (1988) 655–661.

[5] M.V. Karwe, Y. Jaluria, Numerical simulation of thermal transport associated with a continuously moving flat sheet in materials processing, ASME J. Heat Transfer 113 (1991) 612–619.

[6] B.C. Sakiadis, Boundary layer behavior on continuous solid surfaces: I. boundary-layer equations for two-dimensional and axisymmetric flow, A.I.Ch.E. Journal 7 (1) (1961) 26–28.

[7] F.K. Tsou, E.M. Sparrow, R.J. Goldstein, Flow and heat transfer in the boundary layer on a continuous moving surface, Int. J. Heat Mass Transfer 10 (1967) 219–235.

[8] L.J. Crane, Flow past a stretching plane, Z. Amgew. Math. Phys. 21 (1970) 645–647.

[9] L.G. Grubka, K.M. Bobba, Heat transfer characteristics of a continuous stretching surface with variable temperature, ASME J. Heat Transfer 107 (1985) 248–250.

[10] V.M. Soundalgekar, T.V. Ramana Murty, Heat transfer past a continuous moving plate with variable temperature, Wärme- und Stoffübertragung 14 (1980) 91–93.

[11] J. Vleggaar, Laminar boundary layer behavior on continuous accelerating surfaces, Chem. Eng. Sci. 32 (1977) 1517–1525.

[12] M.E. Ali, Heat transfer characteristics of a continuous stretching surface, Wärme- und Stoffübertragung 29 (1994) 227–234.

[13] W.H.H. Banks, Similarity solutions of the boundary-layer equations for a stretching wall, J. Mec. Theor. Appl. 2 (1983) 375–392.

[14] M.E. Ali, The effect of suction or injection on the laminar boundary layer development over a stretched surface, J. King Saud Univ. Eng. Sci. 8 (1) (1996) 43–58.

[15] E. Magyari, B. Keller, Heat and mass transfer in the boundary layers on an exponentially stretching continuous surface, J. Phys. D: Appl. Phys. 32 (1999) 577–585.

[16] E. Magyari, B. Keller, Heat transfer characteristics of the separation boundary flow induced by a continuous stretching surface, J. Phys. D: Appl. Phys. 32 (1999) 2876–2881.

[17] L.E. Erickson, L.T. Fan, V.G. Fox, Heat and mass transfer on a moving continuous flat plate with suction or injection, Ind. Eng. Chem. Fundam. 5 (1966) 19–25.

[18] V.G. Fox, L.E. Erickson, L.T. Fan, Methods for solving the boundary layer equations for moving continuous flat surfaces with suction and injection, A.I.Ch.E. Journal 14 (1968) 726–736.

[19] P.S. Gupta, A.S. Gupta, Heat and mass transfer on a stretching sheet with suction or blowing, Can. J. Chem. Eng. 55 (6) (1977) 744–746.

[20] C.K. Chen, M.I. Char, Heat transfer of a continuous stretching surface with suction or blowing, J. Math. Anal. Appl. 135 (1988) 568–580.

[21] M.E. Ali, On thermal boundary layer on a power-law stretched surface with suction or injection, Int. J. Heat Fluid Flow 16 (4) (1995) 280–290.

[22] E. Magyari, M.E. Ali, B. Keller, Heat and mass transfer characteristics of the self-similar boundary-layer flows induced by continuous surface stretched with rapidly decreasing velocities, Heat Mass Transfer 38 (2001) 65–74.

[23] E. Magyari, B. Keller, Exact solutions for self-similar boundary-layer flows induced by permeable stretching walls, Eur. J. Mech. B-Fluids 19 (2000) 109–122.

[24] H.T. Lin, K.Y. Wu, H.L. Hoh, Mixed convection from an isothermal horizontal plate moving in parallel or reversely to a free stream, Int. J. Heat Mass Transfer 36 (1993) 3547–3554.

[25] B.H. Kang, Y. Jaluria, Heat transfer from continuously moving material in channel flow for thermal processing, J. Thermophys. Heat Transfer 8 (1994) 546–554.

[26] B.H. Kang, Y. Jaluria, Thermal modeling of the continuous casting process, J. Thermophys. Heat Transfer 7 (1) (1993) 139–147.

[27] D.B. Ingham, Singular and non-unique solutions of the boundary-layer equations for the flow due to free convection near a continuously moving vertical plate, Appl. Math. Phys. (ZAMP) 37 (1986) 559–572.

[28] M.E. Ali, F. Al-Yousef, Heat transfer and flow field on an extruded vertical material, in: Proceedings of the 10th International Conference of Mech. Power Engineering, Assiut University, Assiut, Egypt, 16–18 December, 1997, pp. 207–219.

[29] M.E. Ali, F. Al-Yousef, Laminar mixed convection from a continuously moving vertical surface with suction or injection, Heat Mass Transfer 33 (4) (1998) 301–306.

[30] W.M. Kays, M.E. Crawford, Convective Heat and Mass Transfer, third ed., Mcgraw-Hill, New York, 1993.

[31] A. Mucoglu, T.S. Chen, Mixed convection on inclined surfaces, ASME J. Heat Transfer 101 (1979) 422–426.

[32] H. Schlichting, Boundary-Layer Theory, seventh ed., McGraw-Hill, New York, 1979.

[33] A. Bejan, Convection Heat Transfer, Wiley, New York, 1984.